



Effects of Mg content and annealing treatment on optical and electrical properties of CuMg and ITO/CuMg metallic glass films



H.K. Lin*, S.Z. Hong

Graduate Institute of Materials Engineering, National Pingtung University of Science and Technology, Pingtung 912, Taiwan

ARTICLE INFO

Article history:

Received 23 June 2017

Accepted 25 September 2017

Available online 28 September 2017

Keywords:

Laser

Transparent conductive film

Metallic glass

CuMg

Electric resistivity

ABSTRACT

CuMg (CM) and ITO/CuMg (ICM) films with Mg contents ranging from 30 to 65 at% are deposited on glass substrates and are then treated by furnace annealing and laser annealing. The structural, optical and electrical properties of the as-deposited and annealed samples are investigated and compared. It is shown that as the Mg content increases, the sheet resistance of the CM film increases, while the transmittance decreases. For a Mg content of 49 at%, the bi-layer ITO/CM structure improves the transmittance from 62.6% (CM) to 75.6% (ICM) and reduces the resistance from 51.3 Ω/\square (CM) to 49.5 Ω/\square (ICM). Moreover, following furnace annealing at 200 °C, the transmittance of the ICM sample is further improved to 78.5% while the sheet resistance is reduced to 32.4 Ω/\square . The corresponding figure of merit is equal to $2.74 \times 10^{-3} \Omega^{-1}$, and is thus similar to that of commercial ITO film ($2.68 \times 10^{-3} \Omega^{-1}$). The optimal laser annealing parameters for the Cu₅₁Mg₄₉ ICM sample are found to be a pulse energy of 1 μJ and a repetition rate of 250 kHz. Given the use of these parameters, the ICM film has a transmittance of 77.5% and a sheet resistance of 26.5 Ω/\square . The corresponding figure of merit has a value of $2.94 \times 10^{-3} \Omega^{-1}$. Finally, the relative change in resistivity of the as-deposited Cu₄₃Mg₅₇ ICM sample following fatigue testing with a bend radius of 7 mm ($\Delta R/R_0 = 0.21$) is significantly lower than that of a pure ITO film of roughly equivalent thickness ($\Delta R/R_0 = 0.93$).

© 2017 Elsevier B.V. All rights reserved.

1. Introduction

Transparent conducting oxide (TCO) films are widely used for such applications as solar cells, organic light-emitting diodes (OLEDs), touch panels, and flat panel displays [1–3]. Among the various TCO materials available, indium-tin oxide (ITO) is one of the most commonly used due to its low electrical resistivity and high optical transmittance in the visible range. However, to minimize the sheet resistance, the thickness of the ITO film should exceed 100 nm [4,5]. To address this problem, the literature contains many proposals for minimizing the ITO cost by means of doping, sputtering, or a multilayer design [6–8]. In the latter case, the structures typically comprise a middle layer fabricated of a highly-conductive metal such as silver or copper and an upper TCO layer with a thickness of around 5–20 nm. Many studies have shown that such structures yield both good optical transmittance in the visible light range and high electrical conductivity [9–14]. Thin film metallic glasses (TFMGs) have many desirable properties, including a low

surface roughness, high strength, and good mechanical and physical properties [15–18]. Furthermore, the fatigue properties of TFMG hybrid structures are superior to those of commercial monolithic products [19]. As a result, they have found an increasing number of engineering applications in recent years.

Many studies have shown that the optical and electrical properties of thin films can be improved through furnace annealing [20–22]. The literature also contains various proposals for the localized annealing of TCO films using pulsed-laser systems [23–27]. In general, the laser annealing process not only improves the optical and electrical performance of the film, but also reduces the residual stress given a suitable repetition rate [27]. Consequently, the fatigue resistance of the film under bending loads is significantly improved. Furthermore, the fatigue properties of TFMG hybrid structures are superior to those of commercial monolithic products [19].

Lin [28] showed that the optical and electrical properties of MG-based bi-layer films are dependent on both the thickness and the composition of the MG layer. Accordingly, the present study deposits CuMg (CM) monolithic films and ITO/CuMg (ICM) bi-layer films with Mg contents ranging from 30 to 65 at% on glass

* Corresponding author.

E-mail address: HKLin@mail.npust.edu.tw (H.K. Lin).

substrates. The as-deposited CM and ICM films are then treated by furnace annealing and laser annealing. The structures and surface morphologies of the various films are examined by X-ray diffraction (XRD), scanning electron microscopy (SEM) and energy dispersive spectrometry (EDS), respectively. In addition, the optimal annealing processes are determined by evaluating the electrical and optical properties of the samples are evaluated using a four-point probe technique and spectrophotometry, respectively. Finally, the fatigue properties of the ICM samples are examined by means of cyclic bending tests and compared to the performance of commercial products.

2. Experimental

Glass substrates were purchased from Nippon Electric Glass Co. with a thickness of 0.7 mm and an optical transmittance of 92% for an incident wavelength of 550 nm. The CM and ICM films were deposited on the glass substrates using a magnetron sputtering system (Kao Duen Co.) equipped with an ITO target with a composition of 90 wt% In_2O_3 and 10 wt% SnO_2 (ICM films only), a pure Cu target, and a pure Mg target. For all of the samples, the sputtering process was performed using an Ar flow rate of 30 sccm, a base pressure of 2×10^{-6} torr, and a working pressure of 5 mtorr. In every case, CM films with a thickness of 10 nm were deposited on the glass substrate. For the ICM films, an additional ITO layer with a thickness of 30 nm was then sputtered on the CM layer. To evaluate the effects of the composition of the CM layer on the optical and electrical properties of the CM and ICM films, the discharge power of the Cu target was varied in the range of 20–70 W in order to obtain four different CM films, namely $\text{Cu}_{70}\text{Mg}_{30}$, $\text{Cu}_{51}\text{Mg}_{49}$, $\text{Cu}_{43}\text{Mg}_{57}$ and $\text{Cu}_{35}\text{Mg}_{65}$.

The as-deposited CM and ICM films were treated using two different annealing processes, namely furnace annealing and laser annealing. To identify the optimal annealing parameters, the furnace annealing process was performed at various temperatures in the range of 150–300 °C using a heating rate of 5 °C/min and holding an hour in every case. The laser annealing process was carried out using a fiber laser (SPI-12, UK, wavelength 1064 nm) with repetition rates ranging from 100 to 400 kHz and irradiation powers in the range of 42–545 mW. For all of the samples, the laser scanning speed was set as 5 mm/s, the laser spot size as 40 μm , and the pulse duration as 30 ns. The pulse energy (E) was computed as [29]

$$E = P_{\text{AVG}} / \text{rep}, \quad (1)$$

where P_{AVG} and rep denote the average power of the pulse laser and

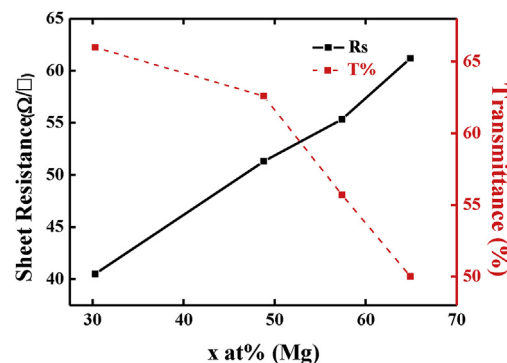
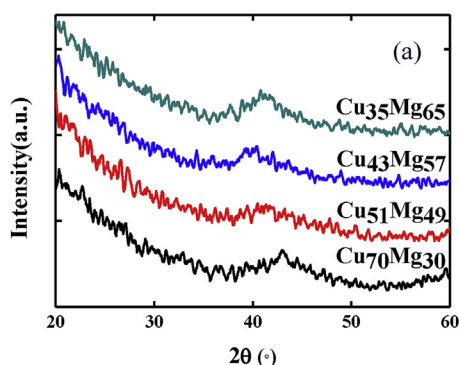


Fig. 2. Sheet resistance and optical transmittance of as-deposited CM films.

the laser repetition rate, respectively. From Eq. (1), it is seen that the pulse energy reduces as the repetition rate increases. For the irradiation powers and repetition rates considered in the present study, the pulse energy varied from 0.5 to 2 μJ .

The morphologies and structure of the as-deposited and annealed films were examined by scanning electron microscopy (SEM, JSM-7600F) and in-plane X-ray diffraction (XRD, Bruker D8 Advance). In addition, the sheet resistance was measured using a four-point probe (SR-H1000C). Finally, the optical transmittance was measured over the range of 200–1100 nm using a UV–vis-IR spectrophotometer (Lambda 35, PerkinElmer).

The performance of the various CM and ICM films was evaluated by means of the following figure of merit [30]:

$$\phi_{\text{TC}} = T^{10}/R, \quad (2)$$

where T is the transmittance (expressed in percentage terms) and R is the sheet resistance (expressed in units of Ω/\square).

The fatigue properties of the as-deposited ICM samples were examined by measuring the change in electrical resistivity of the samples during cyclic bending tests performed with bending curvature radii (R) of 13.5 mm, 15.5 mm and 17.5 mm, respectively. The bending strain ϵ was calculated as

$$\epsilon = hs/2R \times 100\%, \quad (3)$$

where hs is the thickness (PET substrate 50 μm). The bending strain per cycle was therefore equal to 0.36% for bending radii of 7 mm.

3. Results and discussion

Fig. 1(a) shows the X-ray diffraction patterns of the as-deposited

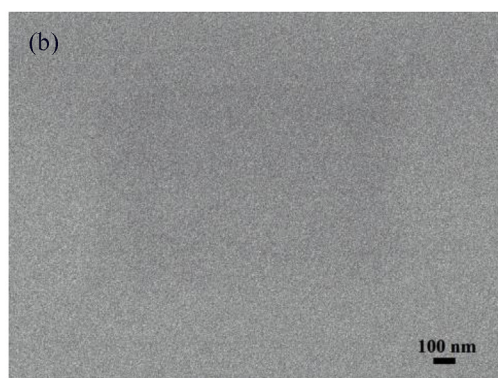


Fig. 1. (a) XRD patterns of CM films, (b) SEM image of $\text{Cu}_{51}\text{Mg}_{49}$ film.

Table 1
Sheet resistance and optical transmittance of as-deposited CM and ICM films.

		Cu ₇₀ Mg ₃₀	Cu ₅₁ Mg ₄₉	Cu ₄₃ Mg ₅₇	Cu ₃₅ Mg ₆₅
CM	Rs	40.5 Ω/□	51.3 Ω/□	55.4 Ω/□	61.2 Ω/□
	T%	66%	62.6%	55.7%	50%
30 nm ITO/		37.8 Ω/□	49.5 Ω/□	52.7 Ω/□	59.8 Ω/□
CM		73.4%	75.6%	72.6%	67%

Cu₇₀Mg₃₀, Cu₅₁Mg₄₉, Cu₄₃Mg₅₇ and Cu₃₅Mg₆₅ films. The absence of any distinct diffraction peaks in the XRD profiles indicates that all of the CM films have an amorphous structure. Moreover, the SEM image of the Cu₅₁Mg₄₉ sample shown in Fig. 1(b) shows that the film surface has a smooth and continuous appearance with no obvious crystalline characteristics. The morphology is similar to that reported for ZrCu deposited on glass substrates [31].

Fig. 2 shows the sheet resistance and optical transmittance of the as-deposited CM samples. It is seen that the sheet resistance increases with an increasing Mg content from 40.5 Ω/□ for the Cu₇₀Mg₃₀ sample to 61.2 Ω/□ for the Cu₃₅Mg₆₅ sample. By contrast, the transmittance of the CM films decreases from 66% to 50% as the Mg content is increased from 30 at% to 65 at%. In general, the results confirm that the electrical and optical properties of the as-deposited CM film are improved given a lower Mg content.

Table 1 shows the sheet resistance and transmittance properties of all the as-deposited CM and ICM films. It is observed that the sheet resistance of the ICM films is lower than that of their CM counterparts. For example, given an Mg content of 30 at%, the ICM film has a sheet resistance of 37.8 Ω/sq, while the CM film has a resistance of 40.5 Ω/sq. For both types of film (i.e., monolithic and bi-layer), the sheet resistance increases with an increasing Mg content. As commented above, the transmittance of the CM films reduces continuously as the Mg content increases. By contrast, for the ICM film, the transmittance increases as the Mg content is increased from 30 to 49 at%, but then decreases as the Mg content is further increased to 65 at%. Overall, the results show that the bi-layer structure improves the optical transmittance by around 11–30% compared to the monolithic films. Fig. 3 shows the figure of merit values of all the as-deposited CM and ICM films. The results confirm that the bi-layer films provide a better electrical and optical performance than the monolithic films. Furthermore, it is seen that of all the films, the Cu₅₁Mg₄₉ ICM film achieves the best overall performance (i.e., a figure of merit equal to $1.23 \times 10^{-3} \Omega^{-1}$).

Table 2 shows the sheet resistance and optical transmittance properties of the furnace annealed ICM bi-layer films. It is seen that for annealing temperatures of 250 °C and 300 °C, the films have a high electrical resistivity; particularly those with a higher Mg content. Of the films annealed at 150 °C and 200 °C, the Cu₅₁Mg₄₉ ICM film annealed at 200 °C has an optical transmittance of 78.5%

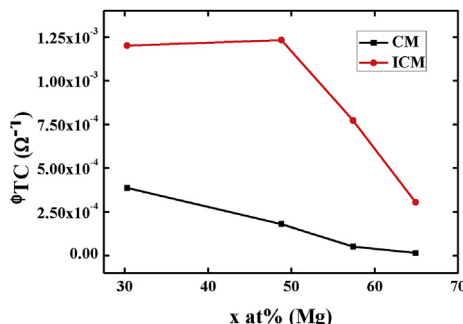


Fig. 3. Figure of merit values of as-deposited CM and ICM films.

Table 2
Sheet resistance and optical transmittance of furnace-annealed ICM films.

		ITO/ Cu ₇₀ Mg ₃₀	ITO/ Cu ₅₁ Mg ₄₉	ITO/ Cu ₄₃ Mg ₅₇	ITO/ Cu ₃₅ Mg ₆₅
150 °C	Rs	32.4 Ω/□	37.8 Ω/□	43.7 Ω/□	52.7 Ω/□
	T%	73.3%	78.2%	78.5%	74%
200 °C	Rs	34.2 Ω/□	32.4 Ω/□	38.7 Ω/□	47.3 Ω/□
	T%	73%	78.5%	79.2%	76.6%
250 °C	Rs	40 Ω/□	31 Ω/□	423 Ω/□	387 Ω/□
	T%	71%	78.1%	76.5%	78.1%
300 °C	Rs	65.7 Ω/□	92.3 Ω/□	495 Ω/□	405 Ω/□
	T%	70.7%	76.7%	77.8%	78.5%

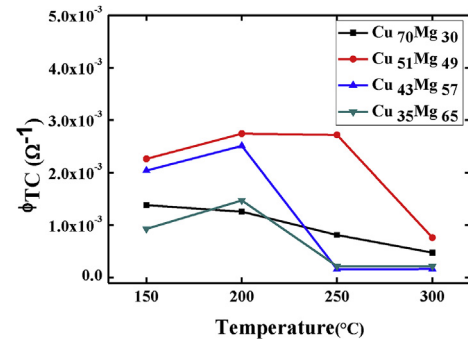


Fig. 4. Figure of merit values of furnace-annealed ICM films.

(representing a 4% improvement over the as-deposited film (75.6%)) and a sheet resistance of 32.4 Ω/□ (representing a 34% improvement over the as-deposited film (49.5 Ω/□)). Fig. 4 shows the figure of merit values of the various furnace annealed ICM films. The results show that the optimal figure of merit ($2.74 \times 10^{-3} \Omega^{-1}$) is obtained by the ICM film with an Mg content of 49 at% and an annealing temperature of 200 °C. It is noted that the figure of merit value is similar to that of commercial ITO film ($2.68 \times 10^{-3} \Omega^{-1}$). Fig. 5(a) and (b) present SEM images of the Cu₄₃Mg₅₇ ICM films annealed at 200 °C and 250 °C, respectively. The surface in Fig. 5(a) has a smooth and continuous characteristic. As a result, the film has a relatively low electrical resistivity (i.e., 38.7 Ω/□, Table 2). However, for the sample annealed at 250 °C (Fig. 5(b)), the surface contains discontinuous island structures as a result of the increased surface energy [32]. Consequently, the film has an extremely high sheet resistance of 423 Ω/□ (Table 2).

Fig. 6 shows the figure of merit values of the various laser-annealed ICM films. As for the furnace-annealed samples, the Cu₅₁Mg₄₉ ICM film achieves the highest figure of merit of the various films for all values of the repetition rate. From inspection, the optimal annealing parameters for the Cu₅₁Mg₄₉ ICM film are seen to be a pulse energy of 1 μJ and a repetition rate of 250 kHz. The resulting figure of merit is equal to $2.94 \times 10^{-3} \Omega^{-1}$.

Fig. 7 presents SEM images of the ICM films annealed using various pulse energies and repetition rates. It is seen that for each film, the surface is discontinuous and contains island structures at higher values of the repetition rate. As described above for the furnace-annealed samples, the formation of these island structures can be attributed to a greater power energy under a higher repetition rate. For the Cu₅₁Mg₄₉ ICM sample, the sheet resistance and transmittance were found to be 26.5 Ω/□ and 77.5%, respectively, given a pulse energy of 1 μJ and a repetition rate of 250 kHz. However, for a higher repetition rate of 400 kHz, the sheet resistance increased to 70.2 Ω/□ as a result of the discontinuous island structures. The figure of merit increased accordingly up to $2.94 \times 10^{-3} \Omega^{-1}$.

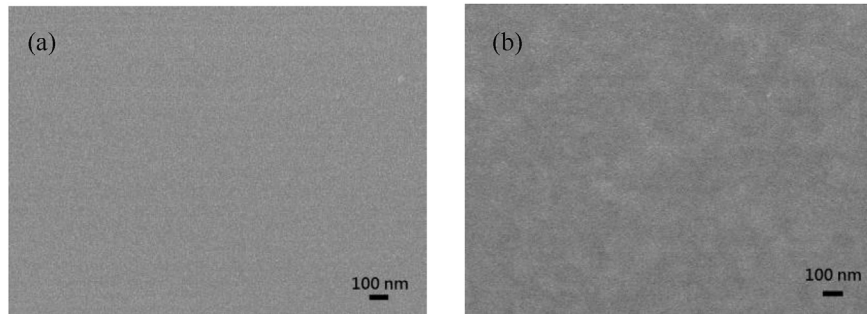


Fig. 5. SEM images of $\text{Cu}_{43}\text{Mg}_{57}$ ICM films furnace annealed at: (a) 200 °C, and (b) 250 °C.

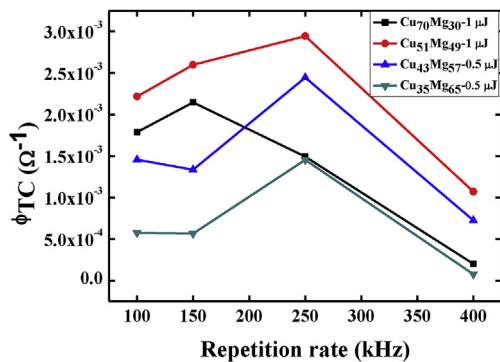


Fig. 6. Figure of merit values of ICM films laser-annealed with different pulse energies and repetition rates.

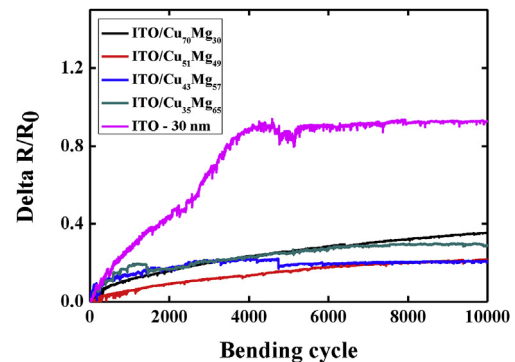


Fig. 8. Relative change in resistivity of as-deposited ICM films and ITO film during fatigue tests performed with bending radii 7 mm.

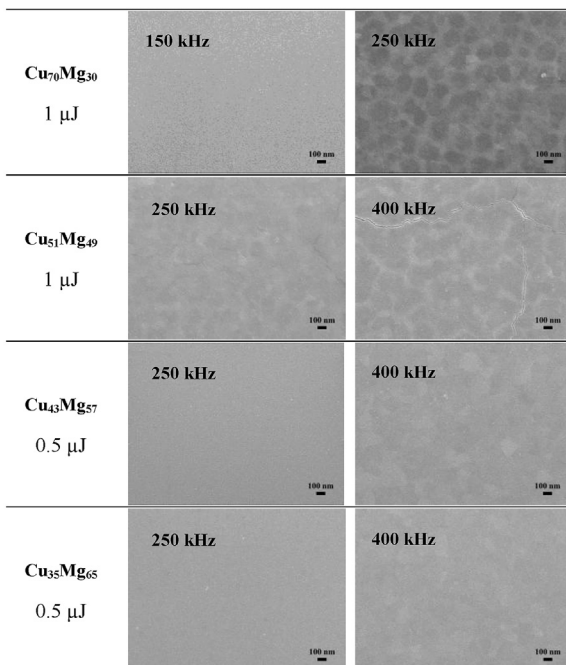


Fig. 7. SEM images of ICM films laser-annealed with different pulse energies and repetition rates.

For ICM films subject to bending fatigue loading, micro-cracks and defects are formed in the microstructure, which result in scattering and degradation of the in-situ electrical resistivity measurements as the number of fatigue cycles increases [19]. In the

present study, the change in electrical resistivity caused by fatigue bending was evaluated as $\Delta R/R_0$, where R_0 is the initial resistivity, R is the measured resistivity after a certain number of fatigue cycles, and ΔR is $R - R_0$. Fig. 8 shows the relative change in resistivity of the as-deposited $\text{Cu}_{70}\text{Mg}_{30}$ ICM, $\text{Cu}_{51}\text{Mg}_{49}$ ICM, $\text{Cu}_{43}\text{Mg}_{57}$ ICM and $\text{Cu}_{35}\text{Mg}_{65}$ ICM samples during bending with radii of curvature 7 mm. For comparison purposes, the results for a pure ITO film with a thickness of 30 nm are also shown. As expected, for each sample, the relative change in resistivity increases with an increasing number of fatigue cycles. However, it is noted that all of the ICM films have a more stable electrical resistivity (i.e., an improved bending fatigue performance) than the pure ITO film. From inspection, the $\Delta R/R_0$ values of the ITO film, $\text{Cu}_{70}\text{Mg}_{30}$ ICM film, $\text{Cu}_{51}\text{Mg}_{49}$ ICM film, $\text{Cu}_{43}\text{Mg}_{57}$ ICM film, and $\text{Cu}_{35}\text{Mg}_{65}$ ICM film are equal to 0.93, 0.35, 0.22, 0.21 and 0.29, respectively, following 10000 bending cycles with a bending radius of 7 mm.

4. Conclusion

It is well known that the optical and electrical properties of MG films depend not only on their thickness, but also on their composition. Accordingly, in the present study, monolithic CuMg (CM) films and bi-layer ITO/CuMg (ICM) films with Mg contents ranging from 30 to 65 at% have been deposited on glass substrates using a magnetron sputtering system. The samples have then been processed using two different annealing treatments, namely furnace annealing and laser annealing. For both treatments, various processing parameters have been considered in order to identify the optimal annealing conditions. The microstructural, optical, electrical and bending fatigue properties of the various samples have then been evaluated and compared.

In general, the results have shown that the as-deposited bi-layer

films have a greater optical transmittance and a lower electrical resistivity than the monolithic films. Of the various as-deposited films, the Cu₅₁Mg₄₉ ICM film achieves the best overall performance, i.e., an optical transmittance of 75.6% and an electrical resistivity of 49.5 Ω/□. The corresponding figure of merit is equal to $1.23 \times 10^{-3} \Omega^{-1}$. The optical and electrical properties of the ICM films are further improved via furnace annealing. For example, given an annealing temperature of 200 °C, the Cu₅₁Mg₄₉ ICM film has an optical transmittance of 78.5% (i.e., 4% higher than the as-deposited film) and a sheet resistance of 32.4 Ω/□ (i.e., 34% lower than the as-deposited film). The corresponding figure of merit is equal to $2.74 \times 10^{-3} \Omega^{-1}$, and is thus slightly higher than that of commercial ITO film ($2.68 \times 10^{-3} \Omega^{-1}$). It has been shown that the optimal laser annealing parameters for the Cu₅₁Mg₄₉ ICM film are a pulse energy of 1 μJ and a repetition rate of 250 kHz. Given the use of these parameters, the film has a transmittance of 77.5% and a sheet resistance of 26.5 Ω/□. The corresponding figure of merit has a value of $2.94 \times 10^{-3} \Omega^{-1}$. Thus, it is inferred that the laser annealing process results in better optical and electrical properties than the furnace annealing process given a Mg content of 49 at%. Finally, it has been shown that all of the ICM films have a better fatigue bending resistance than a pure ITO film of roughly equivalent thickness, and hence provide a more stable electrical response.

Acknowledgement

The authors gratefully acknowledge the financial support provided to this study by the Ministry of Science and Technology of Taiwan under Grant Nos. MOST 105-2221-E-020-007 and 104-2221-E-020-007.

References

- [1] M.H. Ahn, E.S. Cho, S.J. Kwon, Effect of the duty ratio on the indium tin oxide (ITO) film deposited by in-line pulsed DC magnetron sputtering method for resistive touch panel, *Appl. Surf. Sci.* 258 (2011) 1242–1248.
- [2] H.-j. Kim, K.-W. Seo, Y.H. Kim, J. Choi, H.-K. Kim, Direct laser patterning of transparent ITO–Ag–ITO multilayer anodes for organic solar cells, *Appl. Surf. Sci.* 328 (2015) 215–221.
- [3] B.H. Lee, K. Lee Gon, C. Sung Woo, S.-H. Lee, Effect of process parameters on the characteristics of indium tin oxide thin film for flat panel display application, *Thin Solid Films* 302 (1997) 25–30.
- [4] C. Guillén, J. Herrero, Comparison study of ITO thin films deposited by sputtering at room temperature onto polymer and glass substrates, *Thin Solid Films* 480–481 (2005) 129–132.
- [5] J. Lee, H. Jung, J. Lee, D. Lim, K. Yang, J. Yi, W.C. Song, Growth and characterization of indium tin oxide thin films deposited on PET substrates, *Thin Solid Films* 516 (2008) 1634–1639.
- [6] A.H. Ali, A. Shuhaimi, Z. Hassan, Structural, optical and electrical characterization of ITO, ITO/Ag and ITO/Ni transparent conductive electrodes, *Appl. Surf. Sci.* 288 (2014) 599–603.
- [7] K.H. Choi, J.Y. Kim, Y.S. Lee, H.J. Kim, ITO/Ag/ITO multilayer films for the application of a very low resistance transparent electrode, *Thin Solid Films* 341 (1999) 152–155.
- [8] T. Minami, Present status of transparent conducting oxide thin-film development for Indium-Tin-Oxide (ITO) substitutes, *Thin Solid Films* 516 (2008) 5822–5828.
- [9] C. Guillén, J. Herrero, ITO/metal/ITO multilayer structures based on Ag and Cu metal films for high-performance transparent electrodes, *Sol. Energy Mater. Sol. Cell.* 92 (2008) 938–941.
- [10] M. Bendera, W. Seeliga, C. Daubeb, H. Frankenbergerb, B. Ockerb, J. Stollenwerkb, Dependence of film composition and thicknesses on optical and electrical properties of ITO–metal–ITO multilayers, *Thin Solid Films* 326 (1998) 67–71.
- [11] K.H. Choi, J.Y. Kim, Y.S. Lee, H.J. Kim, ITO/Ag/ITO multilayer films for the application of a very low resistance transparent electrode, *Thin Solid Films* 341 (1999) 152–155.
- [12] A. Kloppel, B. Meyer, J. Trube, Influence of substrate temperature and sputtering atmosphere on electrical and optical properties of double silver layer systems, *Thin Solid Films* 392 (2001) 311–314.
- [13] A. Indluru, T.L. Alford, Effect of Ag thickness on electrical transport and optical properties of indium tin oxide–Ag–indium tin oxide multilayers, *J. Appl. Phys.* 105 (2009) 123528.
- [14] C. Guillén, J. Herrero, TCO/metal/TCO structures for energy and flexible electronics, *Thin Solid Films* 520 (2011) 1–17.
- [15] C.W. Chu, J.S.C. Jang, G.J. Chen, S.M. Chiu, Characteristic studies on the Zr-based metallic glass thin film fabricated by magnetron sputtering process, *Surf. Coating. Technol.* 202 (2008) 5564–5566.
- [16] J.P. Chu, J.C. Huang, J.S.C. Jang, Y.C. Wang, P.K. Liaw, Thin film metallic glasses: preparations, properties, and applications, *JOM* 62 (2010) 19–24.
- [17] J.C. Huang, J.P. Chu, J.S.C. Jang, Recent progress in metallic glasses in Taiwan, *Intermetallics* 17 (2009) 973–987.
- [18] J.P. Chu, J.S.C. Jang, J.C. Huang, H.S. Chou, Y. Yang, J.C. Ye, Y.C. Wang, J.W. Lee, F.X. Liu, P.K. Liaw, Y.C. Chen, C.M. Lee, C.L. Li, C. Rullyani, Thin film metallic glasses: unique properties and potential applications, *Thin Solid Films* 520 (2012) 5097–5122.
- [19] H.K. Lin, S.M. Chiu, T.P. Cho, J.C. Huang, Improved bending fatigue behavior of flexible PET/ITO film with thin metallic glass interlayer, *Mater. Lett.* 113 (2013) 182–185.
- [20] D.R. Sahu, C.Y. Chen, S.Y. Lin, J.-L. Huang, Effect of substrate temperature and annealing treatment on the electrical and optical properties of silver-based multilayer coating electrodes, *Thin Solid Films* 515 (2006) 932–935.
- [21] H. Morikawa, M. Fujita, Crystallization and electrical property change on the annealing of amorphous indium-oxide and indium-tin-oxide thin films, *Thin Solid Films* 359 (2000) 61–67.
- [22] I.Y.Y. Bu, A simple annealing process to obtain highly transparent and conductive indium doped tin oxide for dye-sensitized solar cells, *Ceram. Int.* 40 (2014) 3445–3451.
- [23] S.M.d. Nicolás, D. Muñoz, C. Denis, J.F. Lerat, T. Emeraud, Optimisation of ITO by excimer laser annealing for a-Si:H/c-Si solar cells, *Energy Procedia* 27 (2012) 586–591.
- [24] M.F. Chen, K.M. Lin, Y.S. Ho, Laser annealing process of ITO thin films using beam shaping technology, *Optic Laser. Eng.* 50 (2012) 491–495.
- [25] H. Lu, Y. Tu, X. Lin, B. Fang, D. Luo, A. Laaksonen, Effects of laser irradiation on the structure and optical properties of ZnO thin films, *Mater. Lett.* 64 (2010) 2072–2075.
- [26] C.J. Lee, H.K. Lin, C.H. Li, L.X. Chen, C.C. Lee, C.W. Wu, J.C. Huang, A study on electric properties for pulse laser annealing of ITO film after wet etching, *Thin Solid Films* 522 (2012) 330–335.
- [27] H.K. Lin, W.C. Hsu, Electrode patterning of ITO thin films by high repetition rate fiber laser, *Appl. Surf. Sci.* 308 (2014) 58–62.
- [28] H.K. Lin, K.C. Cheng, J.C. Huang, Effects of laser annealing parameters on optical and electrical properties of ITO/metallic glass alloy Bi-layer films, *Nanoscale Res. Lett.* 10 (2015) 982.
- [29] B.R. Benware, C.D. Macchietto, C.H. Moreno, J.J. Rocca, Demonstration of a high average power tabletop soft X-Ray Laser, *Phys. Rev. Lett.* 81 (1998) 5804–5807.
- [30] G. Haacke, New figure of merit for transparent conductors, *J. Appl. Phys.* 47 (1976) 4086.
- [31] C.J. Lee, H.K. Lin, S.Y. Sun, J.C. Huang, Characteristic difference between ITO/ZrCu and ITO/Ag bi-layer films as transparent electrodes deposited on PET substrate, *Appl. Surf. Sci.* 257 (2010) 239–243.
- [32] X. Cen, X. Zhang, A.M. Thron, K. van Benthem, Agglomeration and long-range edge retraction for Au/Ni bilayer films during thermal annealing, *Acta Mater.* 119 (2016) 167–176.